TURKISH JOURNAL of ONCOLOGY

Turk J Oncol 2024;39(2):227–233
doi: 10.5505/tjo.2024.4242

ORIGINAL ARTICLE

Radiation Dosimetry Results for Nitinol: An Experimental Study

Alaattin ÖZEN,[1,2] Kerem DURUER,[3] Helin İSMET[4]

[1]Department of Radiation Oncology, Üsküdar University Faculty of Medicine, İstanbul-*Türkiye*
[2]Comprehensive Cancer Center, Hisar Hospital Intercontinental, İstanbul-*Türkiye*
[3]Department of Radiation Oncology, Eskisehir Osmangazi University Faculty of Medicine, Eskisehir-*Türkiye*
[4]Eskişehir Technical University, Faculty of Architecture and Design, Eskisehir-*Türkiye*

OBJECTIVE

Shape-memory polymers (SMPs) are smart materials suitable for modifying size, shape, stiffness, and strain in response to different external stimuli. Nitinol, used in the medical field, has increased in recent years and is the most important example of SMPs. In this study, we aimed to make the dosimetric evaluation of Nitinol to test its usability in Brachytherapy treatment.

METHODS

To achieve the aim of the study, we designed a tandem to be made of polyamide 12 for the straight part (4 and 6 centimeters on both sides) and Nitinol for the angled part (4 centimeters). Afterward, we placed the produced tandem into the bolus and measured the dose using different dosimetry methods such as the treatment planning system (TPS), GafChromic film dosimetry, and MOSFET dosimetry. Three different measurements were made with the same irradiation dose for each measurement method, and the average results were recorded.

RESULTS

The Euclidean distance between the source and the measuring point was 34.0 millimeters for the Polyamide 12 part, and 32.8 millimeters for the Nitinol part. The calculated irradiation time was 284.9 seconds for the Polyamide 12 part and 268.2 seconds for the Nitinol part. Considering the irradiation times and source distances, the calculated difference between Nitinol and Polyamide 12 was 1.15%. This difference was 1.0%, 1.87%, and 2.08% for TG43, MOSFET, and GafChromic film dosimetry, respectively.

CONCLUSION

In conclusion, Nitinol did not have a negative effect on the dose distribution. However, these results should be supported by further studies including other dosimetry measurements.

Keywords: Brachytherapy; gafchromic film dosimetry; MOSFET dosimetry; nitinol.

INTRODUCTION

Shape-memory polymers (SMPs) are defined as smart materials suitable for modifying size, shape, stiffness, and strain in response to different external stimuli such as heat, electric and magnetic fields, water, or light, similar to pH, body temperature, and ions. The most important feature of SMPs is their ability to return to

This study has been presented as a poster at the American Brachytherapy Society Annual Meeting in 22–24 June 2022.

Received: November 28, 2023
Revised: February 21, 2024
Accepted: February 25, 2024
Online: March 05, 2024

Accessible online at:
www.onkder.org

Dr. Alaattin ÖZEN
Üsküdar Üniversitesi Tıp Fakültesi,
Radyasyon Onkolojisi Anabilim Dalı;
Hisar Hastanesi Kıtalararası,
Kapsamlı Kanser Merkezi,
İstanbul-Türkiye
E-mail: dralovettin@gmail.com

Turk J Oncol 2024;39(2):227–233
doi: 10.5505/tjo.2024.4242

their original shape in the absence of the stimulus without any help. Because of these excellent features, SMPs have received great attention in various fields and are increasingly used in many areas such as sensors, smart textiles, aerospace, robotics, and biomedicine.[1–3]

The most studied SMP types are thermally induced forms. Melting and glass transition temperatures are the main two thermal transition factors underlying the mechanism. As a result of direct thermal application higher than the polymer's transition temperature, the transitory shape of SMP can be programmed. Glass transition temperature-based polymers have a slow shape recovery feature compared to melting temperature-based samples. In addition to this feature, temperatures of glass transitions near physiological body temperature are appropriate properties for biomedical applications.[4–6]

Nitinol is an alloy that contains Nickel (Ni), the seventh most abundant transition metal with face-centered cubic (FCC) coordination, and the twenty-second most abundant element in the earth's crust, Titanium (Ti), a transition metal. Nitinol deforms at low temperatures and returns to its predetermined shape when heated above its transformation temperature. The most important feature of superelastic 55Ni-45Ti tubes is that they can be bent ten times more than steel tubes without kinking or collapsing. Because superelastic Nitinol tubes can be bent ten times more than steel tubes without kinking or collapsing, and combined with wide biocompatibility, Nitinol is used for manufacturing microsurgical equipment. Several manufacturing methods of Nitinol have been developed, such as melting, fabrication, forming, machining, joining, finishing, coating, powder processes, and thin film. Developments in laser cutting, forming, photochemical etching, or surface finishing technologies have improved the physical and mechanical properties of Nitinol. The control of surface finish and corrosion resistance plays a key role in medical implants.[7–11]

In this study, we aimed to make the dosimetric evaluation of Nitinol to test its usability in Brachytherapy treatment.

MATERIALS AND METHODS

Preparation of the Tandem for Experimental Measurement

For the study's purpose, a Nitinol material tube allowing the passage of radioactive material and a tandem made of polyamide 12 (PA 12) material, stably holding this tube, were designed. A Multi Jet Fusion (MJF) 3D printer was used for the part of the tandem to be produced from PA 12 (Fig. 1). For the dimensions envisaged in the technical drawings, the standard precision in production was ±0.3% (±0.1 mm lower limit), layer thickness was 0.08 mm, minimum wall thickness was 0.5 mm, and the print resolution was 1200 dpi.

Dose Measurement

Three different dosimetry methods were used during the dose measurements of the prototype produced (treatment planning system (TPS) for virtual, Radiochromic Film Dosimeter System (EBT3 model, Ashland Specialty Ingredients, Bridgewater, NJ, USA), and Mosfet Dosimeter (Best Medical Canada) system for actual). To use these dosimetric methods, the calibration of the Radiochromic Film Dosimeter System and Mosfet Dosimeter systems was first performed. The distance of the measuring points was chosen completely randomly from TPS, and the Euclidean distance of the measuring point for the Polyamide 12 and Nitinol sections of the tandem was 34.0 and 32.8 mm, respectively.

Radiation Delivery

Planning was made using ACUROS BV and TG43-based calculation algorithms to obtain a dose of 3.0 Gy by selecting a single source position at the measurement points determined virtually in the Treatment Planning System, and the dose values obtained from both algorithms were recorded. At the times calculated with the ACUROS BV calculation algorithm, firstly, the MOSFET detector (Fig. 2) and then the EBT3 film (Fig. 3) were irradiated separately, and the obtained measurement values were recorded. We used an Iridium-192 radioactive source. The source activity was 8,757 curie, and the calculated irradiation duration was 284.9 seconds for the PA12 part and 268.2 seconds for the Nitinol part.

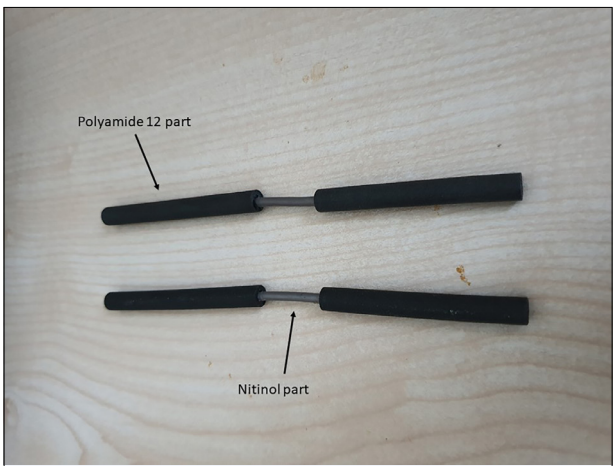

Fig. 1. Produced applicator.

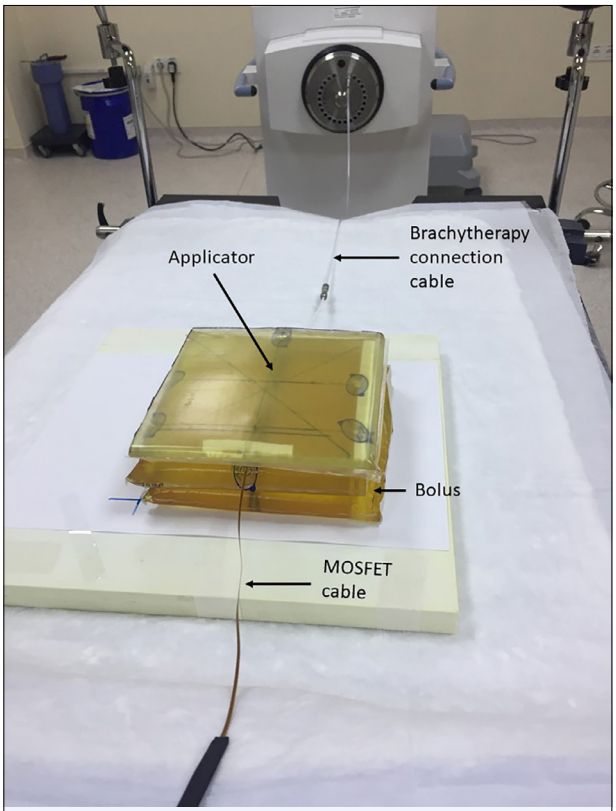

Fig. 2. MOSFET dosimetry.

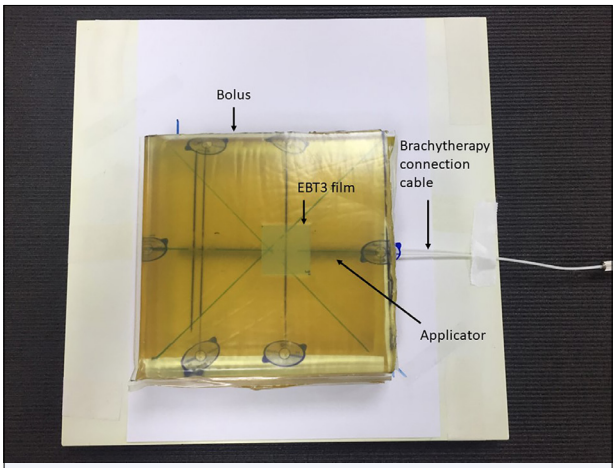

Fig. 3. Film dosimetry.

Statistical Analysis

Categorical variables were described as counts and percentages (%), whereas continuous variables were described as means (±standard deviation). The correlations (r values) were assessed using Pearson's correlation coefficient. All tests of significance were two-tailed with a p-value <0.01.

RESULTS

In the Treatment Planning System, dose definition was made at a fixed point with two different algorithms. After that, irradiation was conducted for the calculated time to obtain this dose, and measurements were taken using MOSFET and GAFchromic film dosimetry. This time was calculated as 283.9 seconds for Polyamide 12 and 268.2 seconds for Nitinol. During these periods, which were calculated using the ACUROS BV calculation algorithm, the MOSFET detector and the EBT3 film were irradiated separately, and the measurement results are given in Table 1. For the Polyamide 12 part, 320±6.6 cGy was measured using the MOSFET dosimetry, and 316.8±3.4 cGy was measured using the GAFchromic film dosimetry, while a dose value of 326±3.6 cGy was measured using the MOSFET dosimetry and 324.7±3.4 cGy was measured using the GAFchromic film dosimetry for the Nitinol part. The values obtained from the TPS and the measurements we made are given in Figure 4 and Figure 5, and the values obtained for the tandem and cylinder parts of the applicator were evaluated in correlation with each other (Table 2).

DISCUSSION

Advancements in radiotherapy today have been characterized by increasingly conformal treatment. The aim of radiotherapy in the modern era is to spare healthy tissue while delivering a biologically effective dose to the target. The advantage of highly conformal techniques is the delivery of a higher dose per fraction over fewer fractions. Brachytherapy refers to the placement of radioactive sources within, or in direct proximity to, the tumor and is the original form of highly targeted radiotherapy. It allows for local dose intensification greater than what can typically be achieved with external beam radiotherapy (EBRT). Prostate cancer, gynecologic cancers, breast cancers, head and neck cancers, and skin cancers are the sites that are frequently treated with brachytherapy.[12]

Although the standard of treatment in patients with endometrial cancer is upfront surgery, several newly diagnosed patients are unable to undergo surgery because of medical comorbidities. In this situation, radiation therapy can be used in patients with early-stage disease for definitive management, in patients with locally advanced disease for preoperative treatment, or for the palliation of symptoms. Historically, low-dose-rate

Turk J Oncol 2024;39(2):227–233
doi: 10.5505/tjo.2024.4242

Table 1 Measurement results obtained for the Polyamide 12 and Nitinol parts of the tandem

Part of tandem	Treatment planning system (cGy)		Duration of irradiation (second)	Distance between source and measurement (mm)	MOSFET (cGy)	GAFchromic film dosimetry (cGy)
	ACUROS BV	TG43				
Polyamide 12	300	316.7	284.9	34.0	320±6.6	316.8±3.4
Nitinol	300	319.3	268.2	32.8	326±3.6	324.7±3.4

Tablo 2 Correlation of dose values obtained from the Treatment Planning System with each other

	Nitinol		Polyamide 12	
	TG43	ACUROS BV	TG43	ACUROS BV
Nitinol				
TG43				
Pearson correlation				
Sig. (2-tailed)				
N				
ACUROS BV				
Pearson correlation	0.998**			
Sig. (2-tailed)	0.000			
N	152			
Polyamide 12				
TG43				
Pearson correlation	1.000**	0.999**		
Sig. (2-tailed)	0.000	0.000		
N	152	152		
ACUROS BV				
Pearson correlation	0.999**	0.999**	0.999**	
Sig. (2-tailed)	0.000	0.000	0.000	
N	152	152	153	

**: Correlation is significant at the 0.01 level (2-tailed)

(LDR) or high-dose-rate (HDR) techniques have been used in combination with EBRT and/or alone in appropriately selected patients. Advances in imaging and radiation therapy technology in recent years have allowed for a more precise definition of tumor targets and the potential for increased accuracy of dose delivery.[13]

The number of applicators that can be used in the brachytherapy treatment of patients with endometrial cancer who cannot undergo surgery is limited.[14–18] For this reason, new brachytherapy applicators that can be used in patients with medically inoperable endometrial cancer need to be developed. Recently, Nitinol, an important biomaterial widely used in the biomedical field, including orthopedics, vascular stents, orthodontics, and other medical devices, has been the subject of this study. Nitinol has unique characteristics, including the shape memory effect, superelasticity, and high damping.[19]

To evaluate the compatibility of the dose calculated in the Treatment Planning System with the doses obtained using different measurement methods, first of all, the factors affecting the dose, which are time (directly proportional), distance (inversely proportional to the square), and activity (directly proportional) values, should be known. The activity during irradiation directly affects the duration, and the Treatment Planning System updates the calculated duration by taking into account the activity of the source (vertical factor). Therefore, the activity was ignored in the evaluation. Since measurements will be made at different thick-

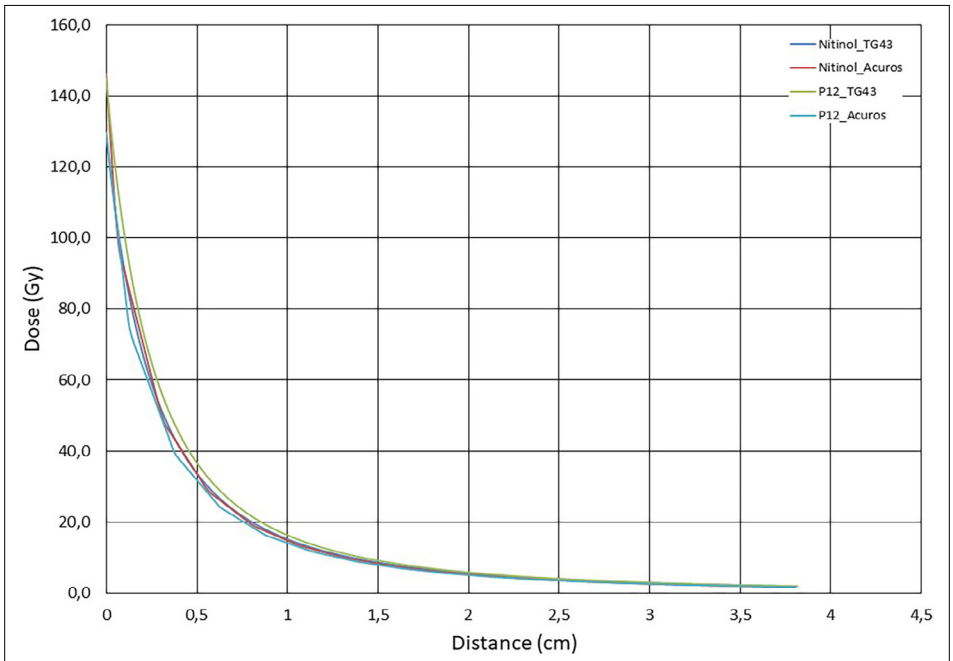

Fig. 4. The relationship between the dose values obtained from the Treatment Planning System and the distance

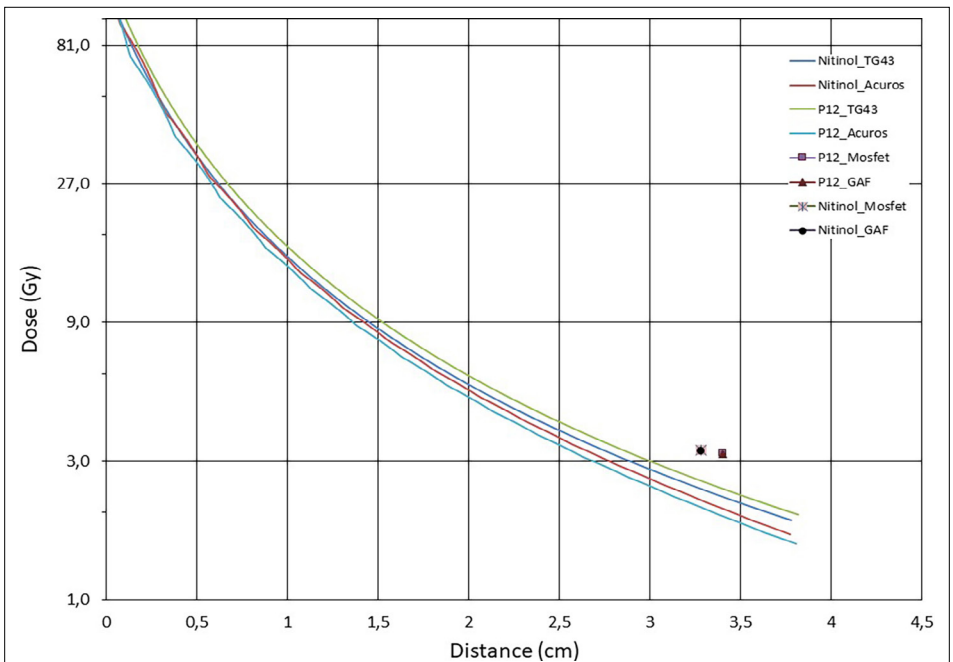

Fig. 5. The relationship between the dose values obtained from the Treatment Planning System and the distance and the correspondence of the dose values obtained as a result of the measurements on the graph.

nesses due to the structure of the applicator, the irradiation dose was kept constant, and the uncertainty of one more value in the formulation was eliminated.

When the literature is examined, the percentage of total uncertainty was calculated as 8.4% in low-dose regions (≤100 cGy) and 6.9% in high-dose regions

Turk J Oncol 2024;39(2):227–233
doi: 10.5505/tjo.2024.4242

(>100 cGy) in measurements made with EBT3 film and 192Ir radioactive-derived brachytherapy systems. [20] In different brachytherapy applications where 192Ir radioactive-sourced brachytherapy systems are used, the total % uncertainty in the measurements performed with the MOSFET detector was calculated in the range of 5.7–6.2%.[21,22] From this point of view, the measurement results we obtained were found to be compatible with the literature.

CONCLUSION

In addition to its shape memory function, Nitinol has excellent thermal conductivity. Also, because of its high corrosion resistance and biocompatibility, Nitinol is especially useful in medical devices. As a result of our experimental study, it has been shown in our measurements that Nitinol does not have a negative effect on radiation permeability. In this context, Nitinol can be used in the production of brachytherapy applicators.

Authorship contributions: Concept – A.Ö.; Design – A.Ö., K.D.; Supervision – A.Ö.; Funding – A.Ö.; Materials – A.Ö., K.D., H.İ.; Data collection and/or processing – K.D., H.İ.; Data analysis and/or interpretation – A.Ö., K.D.; Literature search – A.Ö., K.D.; Writing – A.Ö., K.D.; Critical review – A.Ö.

Conflict of Interest: All authors declared no conflict of interest.

Use of AI for Writing Assistance: Not declared.

Financial Support: This study has been supported by The Scientific and Technological Research Council of Türkiye as project number: 220S572.

Peer-review: Externally peer-reviewed.

REFERENCES

1. Jinsong L, Xin L, Yanju L, Shanyi D. Shape-memory polymers and their composites: Stimulus methods and applications. Prog Mater Sci 2011;56:1077–135.
2. Zhang F, Zhang Z, Zhou T, Liu Y, Leng J. Shape memory polymer nanofibers and their composites: Electrospinning, structure, performance, and applications. Front Mater 2015;2:62.
3. Liu Y, Du H, Liu L, Leng J. Shape memory polymers and their composites in aerospace applications: A review. Smart Mater Struct 2014;23:023001.
4. Zare M, Davoodi P, Ramakrishna S. Electrospun shape memory polymer micro-/nanofibers and tailoring their roles for biomedical applications. Nanomaterials 2021;11:933.
5. Hu J, Zhu Y, Huang H, Lu J. Recent advances in shape-memory polymers: Structure, mechanism, functionality, modeling, and applications. Prog Polym Sci 2012;37:1720–63.
6. Small W 4th, Singhal P, Wilson TS, Maitland DJ. Biomedical applications of thermally activated shape memory polymers. J Mater Chem 2010;20(18):3356–66.
7. Otsuka K, Kakeshita T. Science and technology of shape-memory alloys: New developments. MRS Bull 2002;27(2):91–100.
8. Salas D, Cesari E, Van Humbeeck J, Kustov S. Isothermal B2–B19′ martensitic transformation in Ti-rich Ni–Ti shape memory alloy. Scripta Mater 2014;74:64–7.
9. Tong YX, Guo B, Chen F, Tian B, Li L, Zheng YF, et al. Thermal cycling stability of ultrafine-grained TiNi shape memory alloys processed by equal channel angular pressing. Scripta Mater 2012;67(1):1–4.
10. Kustov S, Salas D, Santamarta R, Cesari E, Van Humbeeck J. Isothermal and athermal martensitic transformations in the B2–R–B19′ sequence in Ni–Ti shape memory alloys. Scripta Mater 2010;63(12):1240–3.
11. Xu JL, Jin XF, Luo JM, Zhong ZC. Fabrication and properties of porous NiTi alloys by microwave sintering for biomedical applications. Mater Lett 2014;124:110–2.
12. Lukens JN, Gamez M, Hu K, Harrison LB. Modern brachytherapy. Semin Oncol 2014;41(6):831–47.
13. Schwarz JK, Beriwal S, Esthappan J, Erickson B, Feltmate C, Fyles A, et al. Consensus statement for brachytherapy for the treatment of medically inoperable endometrial cancer. Brachytherapy 2015;14(5):587–99.
14. Potter R, Haie-Meder C. Endometrial cancer. Leuven, Belgium: ACCO; 2002.
15. Dankulchai P, Petsuksiri J, Chansilpa Y, Hoskin PJ. Image-guided high-dose-rate brachytherapy in inoperable endometrial cancer. Br J Radiol 2014;87(1039):20140018.
16. Heyman JRO, Benner S. The radium hemmet experience with radiotherapy in cancer of the uterus: Classification, method of treatment, and results. Acta Radiol 1941;22:12–98.
17. Simon N, Silverstone SM, Roach LC. Afterloading Heyman applicators. Acta Radiol Ther Phys Biol 1971;10:231–8.
18. Cebecik ÖD, Güzelöz Z, Şancı M. Evaluation of vaginal brachytherapy for treating early-stage endometrial cancer according to the European Society of Medical Oncology 2020 risk stratification. Turk J Obstet Gynecol 2022;19(4):308–14.
19. Alipour S, Taromian F, Ghomi ER, Zare M, Singh S, Ramakrishna S. Nitinol: From historical milestones to functional properties and biomedical applications. Proc Inst Mech Eng H 2022;236(11):1595–612.
20. Oare C, Wilke C, Ehler E, Mathew D, Sterling D, Fer-

reira C. Dose calibration of Gafchromic EBT3 film for Ir-192 brachytherapy source using 3D-printed PLA and ABS plastics. 3D Print Med 2019;5(1):3.
21. Carrara M, Tenconi C, Rossi G, Borroni M, Cerrotta A, Grisotto S, et al. *In vivo* rectal wall measurements during HDR prostate brachytherapy with MOSkin dosimeters integrated on a trans-rectal US probe: Comparison with planned and reconstructed doses. Radiother Oncol 2016;118(1):148–53.
22. Carrara M, Romanyukha A, Tenconi C, Mazzeo D, Cerrotta A, Borroni M, et al. Clinical application of MOSkin dosimeters to rectal wall *in vivo* dosimetry in gynecological HDR brachytherapy. Phys Med 2017;41:5–12.